

ARTICLE

Cardiomyocyte Remodeling and Sarcomere Addition after Uniaxial Static Strain In Vitro

Ji-Guo Yu and Brenda Russell

Department of Physiology and Biophysics, University of Illinois at Chicago, Chicago, Illinois

SUMMARY Individual cardiomyocytes are lengthened in dilated cardiomyopathy. However, it is not known how the new sarcomeres are added to preexisting myofibrils. Using a three-dimensional microtextured culturing system, a 10% mechanical static strain was applied to aligned, well-attached cardiomyocytes from neonatal rat. The morphology of the myofibrils and the ends of the myocytes were examined. Disruptions of the sarcomeric pattern for actin showed a progression from weak to intense staining over 4 hr. The lightly stained sarcomeres were common at 1 hr after being strained, peaked at 2 hr, and then subsided. In contrast, the numbers of intensely stained sarcomeres were initially low, peaked at 3 hr, and then began to decline when compared with control values. The myocyte ends showed elongations and convolutions after 3 hr and 4 hr of mechanical strain when observed with α -actinin and *N*-cadherin staining. We suggest that myocytes from neonatal rat hearts remodel by insertion of new sarcomeres throughout the cell length and also by enhancement at the intercalated discs. (J Histochem Cytochem 53:■■■■–■■■■, 2005)

KEY WORDS

heart failure
cell shape regulation
length remodeling
muscle adaptation
eccentric hypertrophy
myofibrillogenesis

CARDIAC HYPERTROPHY is an adaptive response to increased mechanical load (Russell et al. 2000; Frey and Olson 2003). In studying the relationship between mechanical load and cardiac hypertrophy in vitro, silicon elastomers are widely used as flexible cell culture substrates. By using these flat silicon membranes, numerous studies have examined the effect of mechanical forces on randomly oriented cardiomyocytes in cell culture (Zile et al. 1998; Simpson et al. 1999; Zhuang et al. 2000; Wang et al. 2002; Gopalan et al. 2003). However, on flat silicon membranes only a few of the randomly oriented cardiomyocytes are oriented in the direction of the applied vector. Therefore, flat membranes are not ideal for studying the relationship between mechanical load that occurs in vivo and cardiac hypertrophy.

As we strive to understand the functional mechanisms of mechanical transduction at the cellular level, our group has developed a three-dimensional (3D) culturing system of aligned, well-attached cardiomyocytes (Deutsch et al. 2000; Boateng et al. 2003; Motlagh et

al. 2003a,b). Culturing neonatal rat cardiomyocytes on a 3D surface provides an environment for uniform application of mechanical strain to all cells (Mansour et al. 2004). Using this improved culture system of aligned cardiomyocytes, we have demonstrated a restoration of resting sarcomere from the strained length to the natural length after 4 hr of 10% uniaxial static strain. We suggested that the restoration of the sarcomere length was obtained by the addition of new sarcomeres into the preexisting myofibrils. However, our earlier study did not show where and how the new sarcomeres were added.

In the present study, we used the 3D culturing system for rat neonatal cardiomyocytes and applied a 10% static strain to the cells. The mechanical strain was maintained for 1–4 hr, and the cell morphology was examined with immunofluorescent microscopy during this time period. The use of series sampling over a 4-hr time interval allowed us to quantify the changes in cardiomyocyte structure and remodeling.

Materials and Methods

Microfabrication of Textured Surfaces

Textured substrates for cell culture were fabricated as previously described (Deutsch et al. 2000; Motlagh et al. 2003b;

Correspondence to: Brenda Russell, PhD, Department of Physiology and Biophysics (M/C 901), University of Illinois at Chicago, 835 S. Wolcott Avenue, Chicago, IL 60612-7342. E-mail: Russell@uic.edu

Received for publication December 22, 2004; accepted January 7, 2005 [DOI: 10.1369/jhc.4A6608.2005].

Mansour et al. 2004). Briefly, the parylene-textured surface consisted of parallel grooves. The depth of the groove was 5 μm and spacing between grooves was 10 μm at the top and bottom surfaces. The silicone polydimethylsiloxane membrane was prepared by mixing elastomer and catalyst (A103; Factor II, Inc., Lakeside, AZ) in a 10:1 ratio. The wet mixture was poured over the parylene template and allowed to cure for 2–3 days at room temperature or overnight at 37°C. The silicone membranes were cut into a rectangle (6 \times 3 cm), then peeled and treated with 12 M HCl for 1–2 hr at room temperature. After the acid treatment, the membranes were rinsed two to three times with distilled water and left to dry at 37°C overnight. The membranes were then loaded onto uniaxial static strain devices (Simpson et al. 1999) and soaked in ethanol for at least 1 hr followed by exposure to UV light in the hood for 1 hr to sterilize the surface. The membranes were then rinsed with Moscona's saline (136.8 mM NaCl, 28.6 mM KCl, 11.9 mM NaHCO_3 , 9.4 mM glucose, 0.08 mM NaH_2PO_4 , pH 7.4) and incubated in a solution of fibronectin (10 $\mu\text{g}/\text{ml}$) in Dulbecco's Modified Eagle's Medium (DMEM) nutrient mixture (Sigma; St Louis, MO) for 2 hr at 37°C in a 5% CO_2 incubator. The fibronectin-coated membranes were rinsed with warm Moscona's saline before cell plating.

Cell Culture

Animal experiments were performed according to Institutional Animal Care and Use Committee and NIH guidelines. Cardiomyocytes were isolated from neonatal Sprague-Dawley rats (Harlan; Indianapolis, IN) as previously described (Boateng et al. 2003). Briefly, hearts were removed from 1- to 2-day-old rats. Myocytes were isolated from ventricles and plated on fibronectin-coated silicone membranes (200,000 cells/ cm^2) and maintained in complete medium (DMEM and F-12 HAM without L-glutamine; Sigma), standard amino acid concentrations plus palmitic (2.56 mg/L) and linoleic (0.84 mg/L) fatty acids, penicillin G/streptomycin solution (10 $\mu\text{l}/\text{ml}$), and gentamicin (50 mg/L) with 5% fetal bovine serum for 48 hr before strain experiments.

Mechanical Strain

A strain was applied as previously described (Mansour et al. 2004). Briefly, by manually turning two adjustable screws at the free end of the strain device, a strain of $\sim 10\%$ was applied to longitudinally aligned cardiomyocytes in all experiments. At various time points (1–4 hr) after the imposition of static strain, cells were washed in phosphate-buffered saline (PBS), fixed for 10 min in 4% paraformaldehyde (Fisher), and washed (70% ethanol). After gluing the silicone substrate to a glass slide (4 hr, 25°C) with silicone glue (NuSil

Med 1-4013; NuSil Silicone Technology, Carpinteria, CA), the textured membrane was cut free from the strain device for immunomicroscopy.

Immunohistochemistry

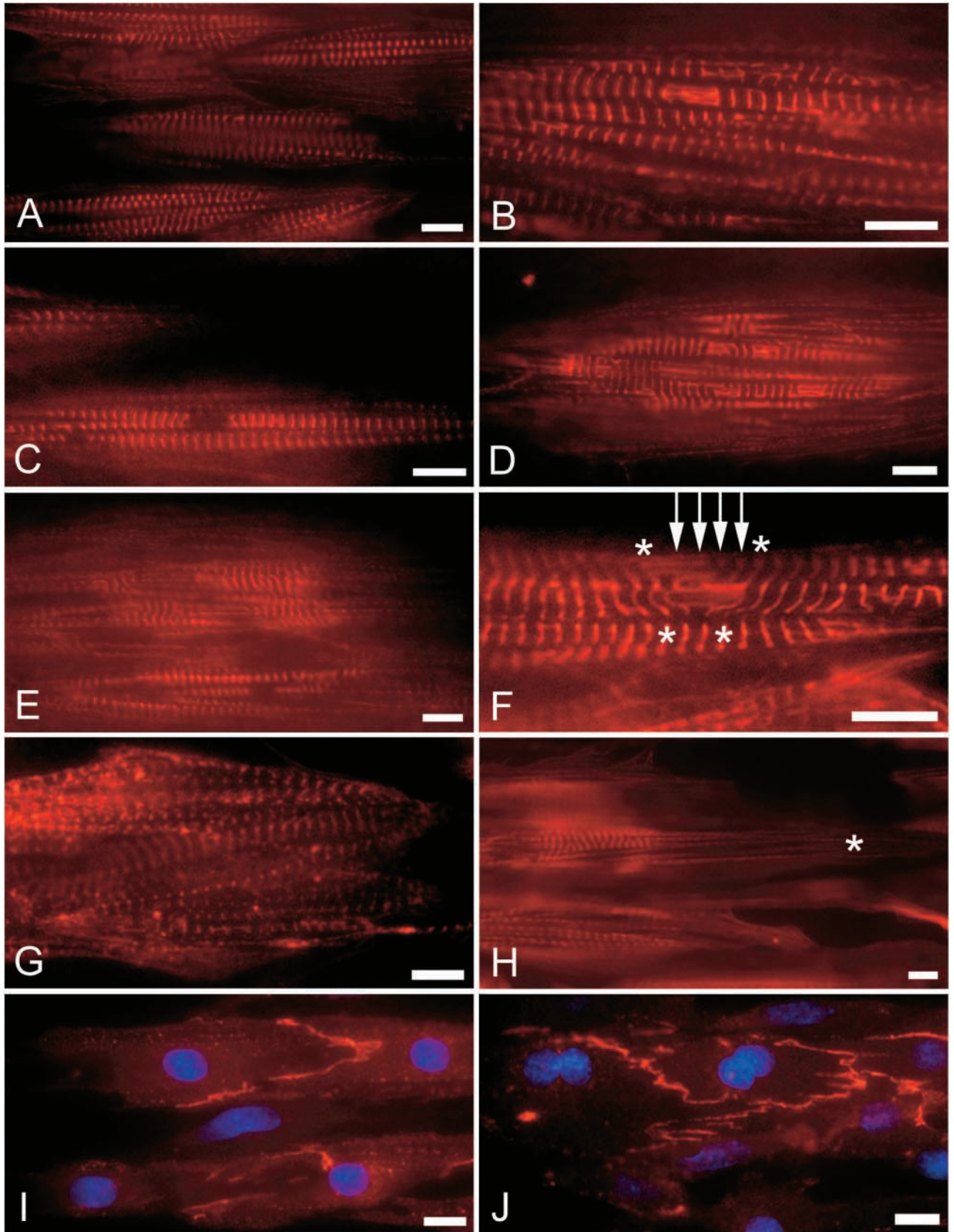
Monoclonal antibodies against α -actinin (EA53; Abcam, Cambridge, MA) and N-cadherin (#32; BD Biosciences, San Jose, CA) were diluted to 1:200 and 1:500, respectively, in 0.01 M PBS containing 0.1% bovine serum albumin. Membranes were incubated with primary antibody for 60 min at 37°C. Visualization of the primary antibody was performed with Alexa-conjugated goat anti-mouse secondary antibody (Molecular Probes; Eugene, OR). Control membranes were treated as above, except that the primary antibody was exchanged with non-immune serum. Filamentous actin was stained with rhodamine phalloidin (Molecular Probes) diluted in PBS (1:20). The membrane was incubated with rhodamine phalloidin for 30 min at room temperature and then rinsed three times (10 min) in PBS. Before applying a coverslip, Vectashield mounting medium (Vector Laboratories; Burlingame, CA) was applied to the surface of the silicone membrane to help preserve the stain. The mounting medium contained DAPI to stain nuclei. Myocytes were observed with a Nikon microscope (Microphot-FXA; Tokyo, Japan) equipped with a Spot RT camera (Diagnostic Instruments; Sterling Heights, MI). Digital images were processed using the Adobe Photoshop 7.0 software (Adobe Systems; Mountain View, CA).

Data Collection and Image Analysis

All membranes were observed using a $\times 60$ objective lens. Ten digital images were taken in a systematic random sample from each membrane. Briefly, the image capturing started from the upper right corner of a membrane, then taking every other visual field in horizontal line scans across the membrane reversing direction when the last field containing cells growing in the grooved surface was reached. Prints were made and coded. All myocytes were carefully examined for any irregular staining by two different investigators who scored the morphological changes by anatomical features and the staining intensity of actin detected by rhodamine phalloidin to reveal the periodic sarcomeric pattern. Structural irregularities were classified into two types and counts recorded: 1. focal areas where the usual sarcomeric pattern was lacking or very weakly stained; 2. focal areas where the usual sarcomeric pattern was intensely stained. After decoding, the morphometric allocation was calculated for the irregular features of control and during the 4 hr after the static strain was applied, which permitted the time course to be determined.

The morphology at the ends of the myocytes after me-

Figure 1 Immunofluorescent staining of rat neonatal cardiac myocytes grown in parallel microgrooves to align them and seen with rhodamine phalloidin (A–F), antibodies against α -actinin (G,H), or N-cadherin (I,J). Myocytes are unstretched (A,G,I) or suddenly stretched 10% and held for 1 (C), 2 (D,E), 3 (B,H,J), and 4 hr (F). Unstretched myocytes showed regular transverse striations (A). After 1 hr (C) and 2 hr (E) of mechanical strain, some myocytes showed focal areas that lacked staining (C) or had wispy longitudinal strands (E). Intensely stained focal areas were seen in single (B,F) and multiple sites (D) in one cell after 2 (D), 3 (B), and 4 hr (F) of strain. Occasionally, a delta-shaped area extends inward from the periphery (F, asterisks with arrows indicating five sarcomeres) to an internal depth (two asterisks, three sarcomeres) suggesting the insertion of two extra sarcomeres. α -Actinin staining showed rounded ends in unstretched myocytes (G), whereas after 3 hr of mechanical strain the ends of the cells narrowed to only one myofibril (H, asterisk). The myocyte junctions after 3 hr of strain were more zigzag or convoluted when stained for N-cadherin (J) compared with unstretched myocytes (I). Bars = 10 μm .



chanical strain was revealed with antibodies against α -actinin and *N*-cadherin. Strain induced pronounced changes for myocytes that terminated in a groove, as well as those abutting another cell at the intercalated disc. The free ends of myocytes were often relatively rounded with many parallel myofibrils having aligned sarcomeres. In other cases, myocytes ended in a relatively sharp point only one myofibril wide. The number of myocytes with rounded vs pointed ends from myocytes stained for α -actinin was counted from coded images as above.

Intercalated discs at myocyte-to-myocyte connections were evaluated by *N*-cadherin staining. These were either fairly straight or they exhibited many zigzags, sharp turns, and a high degree of convolution. The number of myocytes with relatively straight or zigzag features was counted using the double-blind coding as above.

Data Analysis

The number of samples at control, 1, 2, 3, and 4 hr was four. Morphometric counts were averaged for the two observers before computation of statistics. All values are mean \pm SEM. Data were compared using one-way and two-way ANOVA or the Student's unpaired *t*-test. Differences among means were considered significant at $p < 0.05$. Data were analyzed using GraphPad statistical software (GraphPad Software; San Diego, CA).

Results

Sarcomeric Disruptions

The unstretched myocytes stained with rhodamine phalloidin showed regular transverse striations of the I-bands centered on the densely stained Z-disc (Figure 1A). Myocytes that were suddenly stretched and maintained from 1 to 4 hr afterwards with this 10% static strain showed pronounced irregularities in addition to the regular striations. These focal abnormalities in the myofibrils were seen either as weakly stained (Figures 1C and 1E) or intensely stained regions (Figures 1B, 1D, and 1F). The weakly stained areas gave the appearance of a gap in the periodic sarcomeric pattern but close inspection often revealed thin, wispy longitudinal strands connecting the adjacent sarcomeres (Figures 1C and 1E). The length of these myofibrillar interruptions in one cell spanned from only 1 to over 20 μm (or about 10 consecutive sarcomeres). The width of the abnormal region varied from one myofibril to involvement of the entire myocyte (Figures 1C and 1E).

The focal abnormalities stained heavily with rhodamine phalloidin showed thick longitudinal strands (Figures 1B, 1D, and 1F). Such strands generally extended out from the Z-disc and spanned one or more sarcomeres, ending on the Z-disc at the other side of the disrupted region. The number of these focal abnormalities varied from just one per myocyte (Figures 1B and 1F) to several sites (Figure 1D). Most focal irregularities were internally located but occasionally the focal

disruptions began at the edge of a myocyte. One such example on the periphery of a myocyte (Figure 1F) showed increased rhodamine phalloidin staining as a delta-shaped extension so that the peripheral boundary had more sarcomeres than the centrally located area, suggesting that addition of extra sarcomeres had occurred near the cell membrane.

Quantification of the weakly or intensely stained disruptions in the sarcomeres showed the time course for their prevalence over the 4 hr after the static stretch was applied (Figure 2). The lightly stained sarcomeres with apparent gaps in the myofibrils were common at 1 hr after being strained, peaked at 2 hr, and then subsided. In contrast, the numbers of intensely stained sarcomeres were initially low, peaked at 3 hr, and then began to decline when compared with control values. In contrast, the focal areas of intensely stained myocytes was initially low, peaked at 3 hr, and then began to decline when compared with control values

Ends of the Myocytes

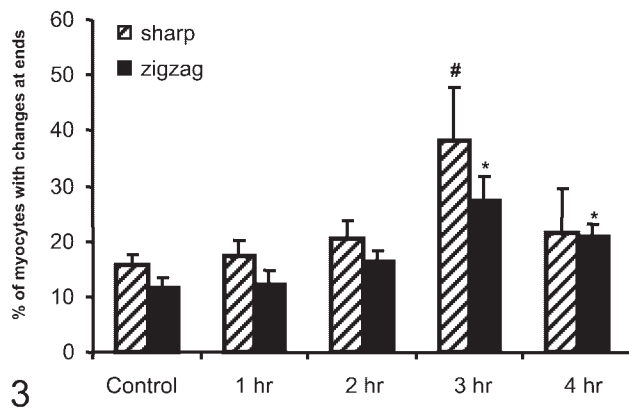
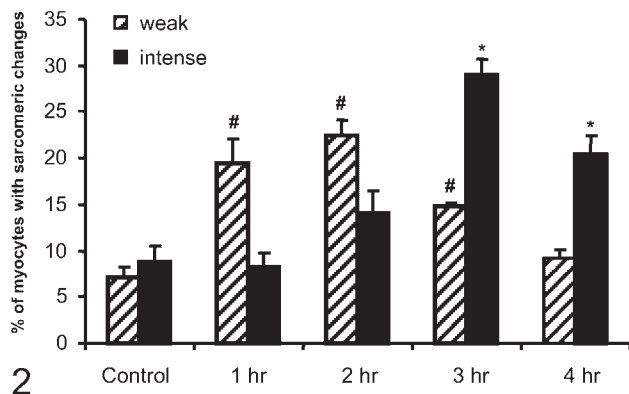
Most of the myocytes densely plated in microgrooves were connected longitudinally by intercalated disks. However, some myocytes had one end free, and occasionally there were isolated myocytes where two free ends were found. α -Actinin was used to reveal the myocyte structure of the intercalated disks as well as the Z-discs at the free ends of myocytes. The morphometric analysis showed that the free ends in the unstretched myocytes generally had two or more myofibrils resulting in a rather rounded tip (Figure 1G). In contrast, myocytes from the mechanically strained cultures had very sharp ends and were usually only one myofibril wide (Figure 1H).

Further details of the myocyte terminations and myocyte-to-myocyte junctions were detected with an antibody against *N*-cadherin. In the unstretched myocytes, the contact between cells was a relatively straight, thin line (Figure 1I). After the mechanical strain, myocytes were coupled by thicker adherent junctions that had many zigzags, sharp turns, and a high degree of convolution (Figure 1J). These anatomic observations were statistically significant at 3 hr and 4 hr of mechanical strain when compared with unstretched myocytes (Figure 3).

Discussion

The 10% static strain resulted in morphological changes in sarcomeres throughout the length of the myofibrils as well as changes at the ends of the myocytes. These changes were interpreted to reflect remodeling of the contractile material in response to the mechanical strain.

A morphometric analysis of the changes in the sarcomeric patterns permits interpretation of a time course for the remodeling events. Initially, 1–3 hr after the



Figures 2 and 3

Figure 2 The percentage of myocytes showing sarcomeric changes. The percentage of myocytes with weakly stained sarcomeres (weak) or apparent gaps was significantly increased after 1, 2, and 3 hr after a sudden 10% static mechanical strain (19.5 ± 2.6 , 22.5 ± 1.7 , and 14.7 ± 0.5 vs 7.1 ± 1.2 , # $p < 0.05$), whereas the percentage of myocytes with intensely stained sarcomeres (intense) was significantly increased after 3 hr and 4 hr of static strain (29.1 ± 1.6 and 20.4 ± 2.1 vs 8.8 ± 1.6 , * $p < 0.05$) when compared with control values.

Figure 3 The percentage of myocytes with changes at the cell ends. Staining for α -actinin revealed myocytes with sharp ends only one myofibril wide (sharp). The percentage of myocytes with sharp ends was significantly increased after 3 hr of mechanical strain when compared with control value (38.3 ± 9.6 vs 15.7 ± 2.0 , # $p < 0.05$). Staining for *N*-cadherin revealed the intercalated discs. The percentage of myocytes with zigzag connections (zigzag) was increased after 3 hr and 4 hr of static strain when compared with control value (27.4 ± 4.5 and 21 ± 2.1 vs 11.4 ± 2.1 , * $p < 0.05$).

application of a sudden strain, the most common changes were the weakly stained gaps along myocytes, whereas in the later period (3 hr and 4 hr) more myocytes showed regions that stained intensely for F-actin. We hypothesize that the mechanical strain disrupts the periodic structure in the myofibril, first leaving the weakly stained gaps. We note that, in some of the gaps, some thin, wispy longitudinal strands survive and appear to connect the adjacent sarcomeres. We suggest that these thin longitudinal F-actin strands might form

a platform for the initiation for repair of the disruption. As the repair progresses, more F-actin filaments might be accumulated, forming the intensely stained regions observed 3–4 hr after straining. Interestingly, within the intensely stained areas, there were some regions where some extra sarcomeres were observed, suggesting that the repair is not simply a reassembly of the original periodic structure but a remodeling process with the addition of new sarcomeres into the pre-existing myofibrils.

Cyclic stresses and strains occur in normal physiology, and when these stresses and strains are maintained at new levels, the myocyte responds by growth or atrophy. Cells elongate in response to increased diastolic strain by adding sarcomeres in series, and they thicken in response to continued stress by adding filaments in parallel (Russell et al. 2000). They do this while still keeping the resting sarcomere length close to its optimal value at the peak of the length-tension curve. One could argue that cells in dilated cardiomyopathy have adapted well to a never-ending volume overload by an obligatory lengthening coupled to mechano-sensing of strain. In contrast, myocytes in concentric myopathy that is short and thick has adapted to overstress (Gerdes et al. 1992). Thus, these shapes eventually become maladapted because long, thin myocytes provide little total force for ejection of the blood whereas short, thick ones intrude on chamber volume itself. We suggest that sarcomerogenesis in the neonatal myocyte induced by mechanical strain in culture might form the basis for increased lengthening of individual cardiomyocytes in dilated cardiomyopathy.

It is possible that costameres and Z-discs in myofiber play a key role for addition of new filaments to existing myofibrils in hypertrophying myocytes. Recent studies in human skeletal muscle confirm that new sarcomeres are added along the entire length of the fiber (Yu and Thornell 2002, Yu et al. 2003,2004). Essentially, a Y-shaped scaffold of desmin is inserted at the costamere permitting new shorter sarcomeres to be spliced into the Z-disk. Quick stretches deform the middle of a muscle to a greater extent because it is less stiff and less well protected than at the ends. Thus, skeletal muscle is weakest in the middle, so new sarcomeres are most likely added centrally as a response to increased stretch (Yu and Thornell 2002, Yu et al. 2003,2004). Cardiac connective tissue is equally strong throughout the length of the cell. Passive resistance is much higher than in skeletal muscle due to titin internally and collagen externally. Despite the differences between skeletal muscle and cardiac tissue, the present study demonstrated that new sarcomeres could also be added at the costameres and central regions (Z-disc) of myofiber in culture but differential resistance in vivo might result in altered morphological insertion sites.

In the present study, the myocytes in the mechani-

cally strained cultures usually had very elongated ends and were only one myofibril wide. Close inspection also revealed that the sarcomeric transverse striations in the myocyte ends were not complete but had regular punctate spots of α -actinin, which might correspond to developing Z-discs.

The intercalated discs in unstretched myocytes follow a straight course between cells, whereas after the mechanical strain more zigzags or convoluted patterns were observed especially at the 3 hr and 4 hr sampling times. We suggest that the zigzag pattern of the intercalated discs might correlate with new sarcomere appearance and yield progressive lengthening at the ends of the cell. The intercalated disc has been suggested to be one of the key structures in heart failure because of its integral function in mechanical force transmission as well as intercellular communication in the heart (Perriard et al. 2003).

In conclusion, our study investigated the remodeling of rat neonatal myocytes after static strain of aligned cells in vitro. Our major finding is the addition of new sarcomeres throughout the entire length of the myofibril and major changes in the irregularity of the intercalated disc at the end of the myocytes.

Acknowledgments

This research is supported by the National Heart, Lung, and Blood Institute, National Institutes of Health Grants HL-64956 and HL-62426 to B.R.

Literature Cited

- Boateng SY, Hartman TJ, Ahluwalia N, Vidula H, Desai TA, Russell B (2003) Inhibition of fibroblast proliferation in cardiac myocyte cultures by surface microtopography. *Am J Physiol Cell Physiol* 285:C171-182
- Deutsch J, Motlagh D, Russell B, Desai TA (2000) Fabrication of microtextured membranes for cardiac myocyte attachment and orientation. *J Biomed Mater Res* 53:267-275
- Gerdes AM, Kellerman SE, Moore JA, Muffly KE, Clark LC, Reaves PY, Malec KB, et al. (1992) Structural remodeling of cardiac myocytes in patients with ischemic cardiomyopathy. *Circulation* 86:426-430
- Gopalan SM, Flaim C, Bhatia SN, Hoshijima M, Knoell R, Chien KR, Omens JH, et al. (2003) Anisotropic stretch-induced hypertrophy in neonatal ventricular myocytes micropatterned on deformable elastomers. *Biotechnol Bioeng* 81:578-587
- Frey N, Olson EN (2003) Cardiac hypertrophy: the good, the bad, and the ugly. *Annu Rev Physiol* 65:45-79
- Mansour H, de Tombe PP, Samarel AM, Russell B (2004) Restoration of resting sarcomere length after uniaxial static strain is regulated by protein kinase Cepsilon and focal adhesion kinase. *Circ Res* 94:642-649
- Motlagh D, Hartman TJ, Desai TA, Russell B (2003a) Microfabricated grooves recapitulate neonatal myocyte connexin43 and N-cadherin expression and localization. *J Biomed Mater Res* 67A:148-157
- Motlagh D, Senyo SE, Desai TA, Russell B (2003b) Microtextured substrata alter gene expression, protein localization and the shape of cardiac myocytes. *Biomaterials* 24:2463-2476
- Perriard JC, Hirschy A, Ehler E (2003) Dilated cardiomyopathy: a disease of the intercalated disc? *Trends Cardiovasc Med* 13:30-38
- Russell B, Motlagh D, Ashley WW (2000) Form follows function: how muscle shape is regulated by work. *J Appl Physiol* 88:1127-1132
- Simpson DG, Majeski M, Borg TK, Terracio L (1999) Regulation of cardiac myocyte protein turnover and myofibrillar structure in vitro by specific directions of stretch. *Circ Res* 85:e59-69
- Wang Y, De Keulenaer GW, Weinberg EO, Muangman S, Gualberto A, Landschulz KY, Turi TG, et al. (2002) Direct biomechanical induction of endogenous calcineurin inhibitor Down Syndrome Critical Region-1 in cardiac myocytes. *Am J Physiol Heart Circ Physiol* 283:H533-539
- Yu JG, Carlsson L, Thornell LE (2004) Evidence for myofibril remodeling as opposed to myofibril damage in human muscles with DOMS: an ultrastructural and immunoelectron microscopic study. *Histochem Cell Biol* 121:219-227
- Yu JG, Furst DO, Thornell LE (2003) The mode of myofibril remodeling in human skeletal muscle affected by DOMS induced by eccentric contractions. *Histochem Cell Biol* 119:383-393
- Yu JG, Thornell LE (2002) Desmin and actin alterations in human muscles affected by delayed onset muscle soreness: a high resolution immunocytochemical study. *Histochem Cell Biol* 118:171-179
- Zhuang J, Yamada KA, Saffitz JE, Kleber AG (2000) Pulsatile stretch remodels cell-to-cell communication in cultured myocytes. *Circ Res* 87:316-322
- Zile MR, Cowles MK, Buckley JM, Richardson K, Cowles BA, Baicu CF, Cooper GIV, et al. (1998) Gel stretch method: a new method to measure constitutive properties of cardiac muscle cells. *Am J Physiol* 274:H2188-2202